Arch. Metall. Mater. **67** (2022), 4, 1535-1538

DOI: https://doi.org/10.24425/amm.2022.141089

YU-JIN HWANG[1], KYU-SIK KIM[1,2], JAE-SUNG PARK[3], KEE-AHN LEE[1*]

MANUFACTURE OF MoO_3 COATING LAYER USING THERMAL SPRAY PROCESS AND ANALYSIS OF MICROSTRUCTURE AND PROPERTIES

MoO_3 thick film was manufactured by using a thermal spray process (Atmospheric Plasma Spray, or APS) and its microstructure, phase composition and properties of the coating layer were investigated. Initial powder feedstock was composed of an orthorhombic α-MoO_3 phase, and the average powder particle size was 6.7 μm. As a result of the APS coating process, a MoO_3 coating layer with a thickness of about 90 μm was obtained. Phase transformation occurred during the process, and the coating layer consisted of not only α-MoO_3 but also β-MoO_3, MoO_2. Phase transformation could be due to the rapid cooling that occurred during the process. The properties of the coating layer were evaluated using a nano indentation test. Hardness and reduced modulus were obtained as 0.47 GPa and 1.4 GPa, respectively. Based on the above results, the possibility of manufacturing a MoO_3 thick coating layer using thermal spray is presented.

Keywords: MoO_3; Thermal spray; Atmospheric plasma spray; Microstructure; Properties

1. Introduction

MoO_3 is a transition metal oxide garnering great attention for its electrochromic properties and outstanding catalytic actions [1,2]. Due to such characteristics, it is used in various fields ranging from gas sensors to next-generation anode material for lithium-ion batteries [3-5]. At present, the most common application of MoO_3 is thin film in nm units, and various deposit techniques, including chemical vapor deposition [6], electrophoretic deposition [7], electron beam evaporation [8], sputtering [9] and sol-gel method [10], are used to manufacture MoO_3 film. However, the film that these techniques can manufacture is extremely thin, and they are limited in manufacturing thick films. If a thick film of tens of μm or more is made, it will be possible to use the attractive properties of MoO_3 in new fields.

The thermal spray process is a coating process that deposits metal/non-metal feedstock in a melting or semi-melting state [11]. Unlike other processes that coat the top of a flat substrate, spray coating is capable of evenly coating a substrate with an uneven surface, and it is also capable of manufacturing thick film. The process can be categorized according to its heat source, and among various heat sources, plasma spraying uses plasma created using gas, such as Ar, N_2 and He, as an accelerator to melt and deposit the feedstock on the substrate to form a coating layer [11]. Furthermore, as plasma spray uses a high temperature heat source, it also has an advantage in ceramic coating [12].

When coating a metallic substrate with ceramic using the thermal spray process, massive residual stress and degradation can occur due to the large thermal expansion coefficient difference and rapid temperature change from liquid state to warm solid state during the process. As a result, the coating layer can separate from the substrate [13]. In the case of MoO_3, the emphasis was on manufacturing thin films with thicknesses of nm, so there are almost no studies investigating the manufacturing of coating layers using thermal spray. Golozar et al. used the precursor $(NH_4)_6Mo_7O_{24}\cdot 4H_2O$(ammonium molybdate tetrahydrate) to conduct solution precursor plasma spray(SPPS) and reported that a porous nanocrystalline α-MoO_3 coating layer with a thickness of 15-26 μm was manufactured [14]. Furthermore, the report presented the possibility of utilizing the MoO_3 coating layer as a super-capacitor electrode [14].

This study attempted to manufacture a MoO_3 coating layer with thickness in μm units using the thermal spray process, and investigated the microstructure, phase composition and properties of the manufactured coating layer.

[1] INHA UNIVERSITY, DEPARTMENT OF MATERIALS SCIENCE AND ENGINEERING, INCHEON, KOREA
[2] AGENCY FOR DEFENSE DEVELOPMENT, DAEJEON, KOREA
[3] LT METAL, SEOUL, KOREA

* Corresponding author: keeahn@inha.ac.kr

2. Experimental

This study used MoO_3 powder purchased from Nanografi, with a purity of 3N (99.97 %). Powder morphology was analyzed using FE-SEM (S-4300SE, Hitachi), and the powder size and distribution were analyzed using a laser particle size analyzer (Mastersizer 3000, Malvern PANalytical). The initial powder had a particle size ranging from a few nm to massive particles larger than 100 μm. An X-ray diffractometer (XRD; X'Pert Pro MRD, PANalytical: Cu-Kα, scan step size: 0.02°, scan rate: 1°/min) was used to identify the feedstock's phase composition.

The substrate used for the coating was pure Cu. Before performing coating, Al_2O_3 was used to sandblast the substrate, and a high-pressure air compressor was used to air blow residual particles off the substrate. The plasma spray process was conducted in atmospheric pressure (i.e., atmospheric plasma spray, or APS), and the equipment used was the SG-100 from Praxair. To identify the optimal conditions, various tests were conducted with varying currents and voltages. As a result, all conditions failed to obtain a dense coating layer, and necks were formed through particle surface bonding. The micro-Vickers hardness values of the unsound coating layers measured ranged from 20 Hv to 65 Hv. The reasons for this were analyzed to be i) the size distribution of the feedstock was wide, and ii) the thermal conductivity of MoO_3 was low, causing heat to not transfer properly to the particles. Therefore, additional sieving was performed to reduce the powder size distribution. The above powder feedstock was used for the plasma spray process, and the process conditions were voltage of 45 V, current of 600 A, stand-off distance (SoD) of 100 mm, pitch of 3 mm, powder carrier gas of Ar (10 SCFH) and plasma gas of Ar/N_2 (105/42 SCFH).

FE-SEM was used to observe the cross-sectional microstructure of the coating layer. Before observation, the mounting sample underwent grinding with SiC paper up to #4000, and mirror polishing using 1 μm diamond suspension was applied. Phase analysis of the coating layer was performed using X-ray diffraction (XRD). To investigate the physical properties of the coating layer, a micro-Vickers hardness tester (HM-200, Mitutoyo) and nano indenter (TI-950, Bruker) were used. Ten tests were conducted on each sample, and the average of outcomes was used. The nano indenter test was used to measure the mean hardness and reduced modulus. A Berkovich-type tip was used, and a load of 3mN was applied. In addition, the loading-holding-unloading times were set as 5 sec, 2 sec and 5 sec, respectively.

3. Results and discussion

Fig. 1(a) is the FE-SEM observation of the powder morphology. The powder had an irregular shape. Fig. 1(b) is the X-ray diffraction phase analysis of the initial powder, and which was composed of α-MoO_3 phases with an orthorhombic structure. In addition to the thermally stable orthorhombic α-phase, MoO_3 is reported to also have crystalline phases, such as semi-stable

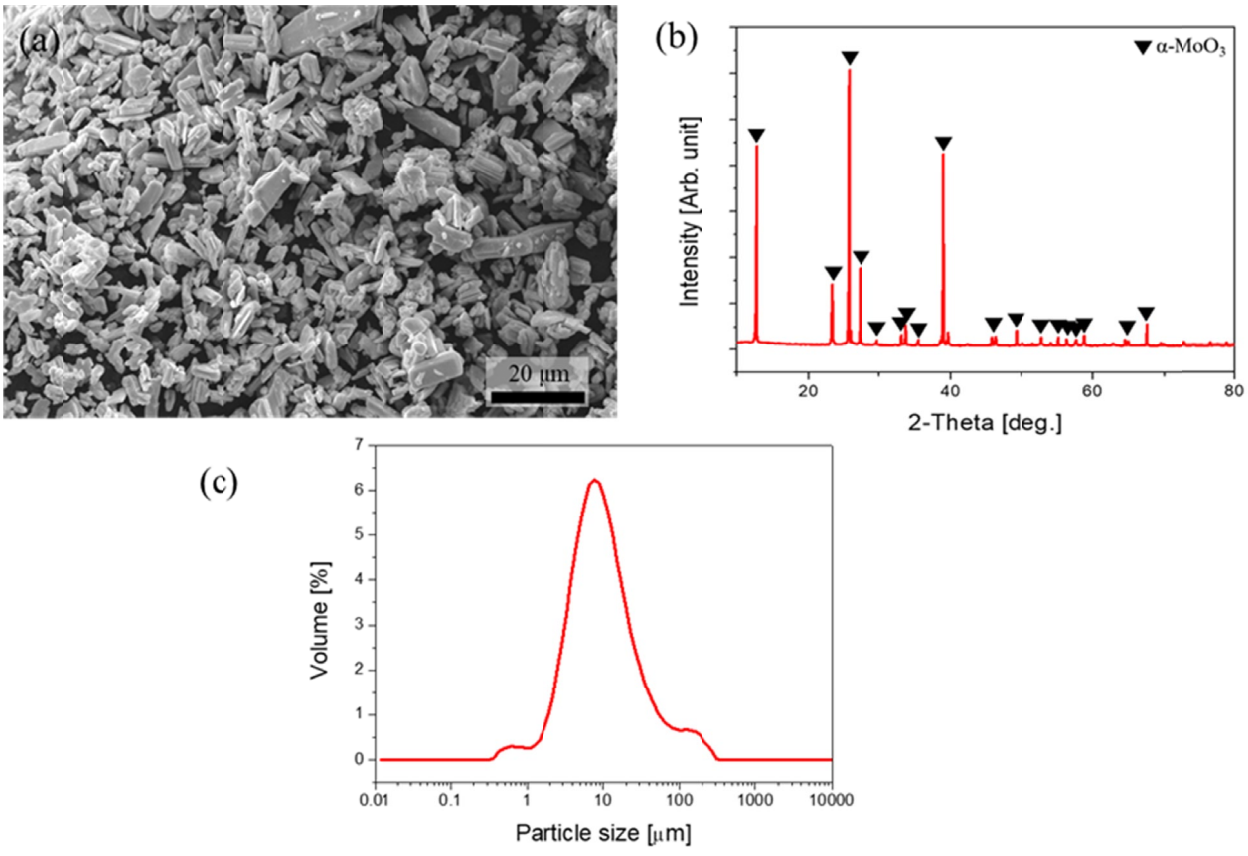

Fig. 1. (a) FE-SEM image, (b) X-ray diffraction graph and (c) size distribution graph of MoO_3 initial powder

monoclinic β-phase and hexagonal h-phase [15]. Fig. 1(c) shows the average powder size and size distribution analysis results. While the initial powder had a relatively narrow distribution, there were still fine particles of nm units. The powder size distribution curve has a bi-modal shape, and the average powder size was 6.7 μm.

The melting point and boiling point of MoO_3 are 795°C and 1155°C, respectively, which are significantly lower than other oxides with high temperature melting points. As a result, the powder easily vaporizes when exposed to high-temperature plasma, so the process was conducted considering that quality of the coating layer can decrease due to such a characteristic. When the process was performed with a constant voltage and different currents during the pre-test, the sample manufactured with the 600 A, 35V conditions had the highest hardness. In many studies, pores present on the coating are known to reduce the hardness of the coating layer as it accepts deformation without resistance [16-18]. Therefore, it is possible to estimate that the process condition with the highest hardness value will be able to manufacture the densest coating layer. Based on the hardness test results of coating layer materials, additional tests were conducted with current fixed at 600 A and the voltage increased to 45 V to improve the quality of the coating layer. With the increased plasma power, the melting level of the powder was expected to increase. A cross-sectional image of the coating layer manufactured with the corresponding process condition was observed using FE-SEM, and the results are presented in Fig. 2. The coating layer was approximately 90 μm thick, and the microstructure was composed of lamellae. In general, the APS process will undergo cooling when melted particles (i.e., droplets) collide, and heat transfer to the substrate causes immediate solidification. As the heat transfer to the substrate is extremely fast, the coating layer undergoes rapid cooling [19], and it is known that the depositing of droplets forms a coating layer composed of lamellae. In addition, the cross-sectional microstructure of the coating layer was confirmed to have defects including inter-lamellar cracks, large pores and unmelted powder. A hardness test was conducted to identify the densification of the coating layer, and the hardness of the coating layer measured 198.4 Hv. This hardness value is approximately three

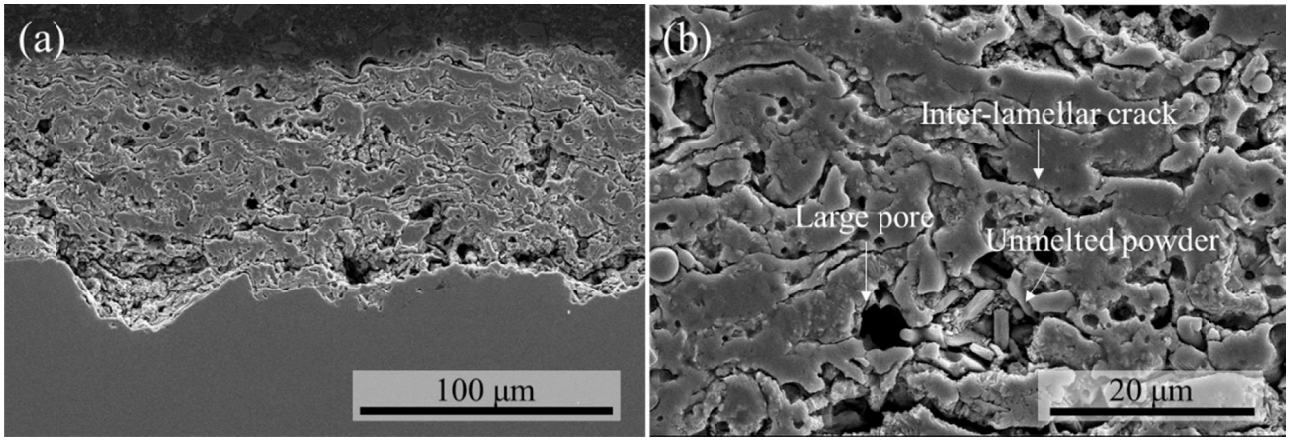

Fig. 2. Cross-sectional FE-SEM images of coating layer; (a) low magnification and (b) high magnification image

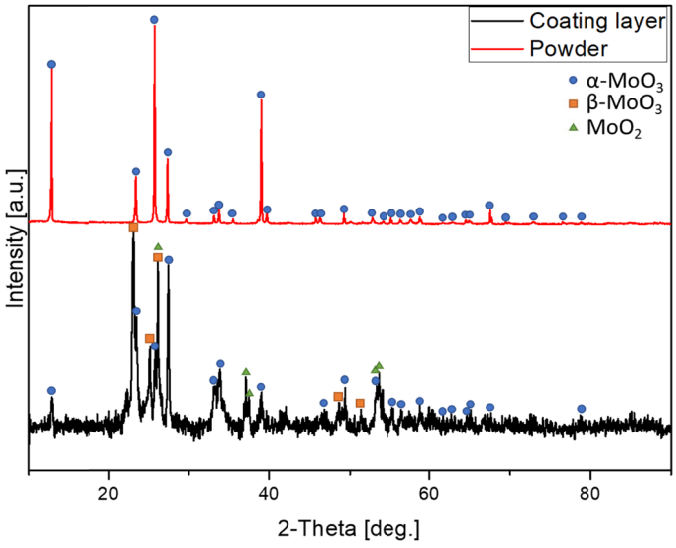

Fig. 3. X-ray diffraction graphs of initial powder and APS coating layer (●: α-MoO_3, ■: β-MoO_3, ▲: MoO_2)

times higher than the hardness value measured for the unsound coating layers formed during pre-tests. This finding confirms the densification increase in the coating layer.

Fig. 3 is the XRD analysis of the coating layer. Unlike the initial powder (Fig. 1(b)), the coating layer was composed of α-MoO_3 phase as well as metastable phase β-MoO_3 phase and MoO_2 phase. In other words, phase transformation occurred during the plasma spray process. And, when those two XRD analysis results between initial powder feedstock (above) and manufactured coating layer (bellow) were compared, the tendency of broad peak baseline from 20 degree to 30 degree appeared in the coating layer. Shahien et al. used the APS process to coat Al_2O_3, and reported the phase analysis results. As the more fully melted powder was used according to SoD, the number of α-Al_2O_3 phases undergoing phase transformation into γ-Al_2O_3 phase increased [20]. This was understood to be the result of rapid cooling that took place when the liquid state shifted to a solid state during the process. Through the findings

of this study, it was estimated that most of the particles fully melted in the corresponding process condition. The occurrence of phase transformation can be explained with the powder particles composed of thermodynamically stable α-MoO_3 phases becoming a liquid state due to the exposure to high temperature plasma and then undergoing rapid cooling as a result of heat transfer to the substrate. And, amorphous phase formation was also suspected to be caused by rapid cooling. In relation to this, Kim et al. reported the possibility of amorphous phase formation in APSed Al_2O_3-ZrO_2 due to rapid cooling [21].

A nano indentation test was conducted to evaluate the properties of the manufactured coating layer (Fig. 4). As pores were present within the coating layer, changes in displacement during holding time were observed in the graph. The test found that the average hardness of the coating layer measured 0.47±0.12 GPa, and the reduced modulus measured 13.4±3.86 GPa. The deviation between hardness values was checked as ~25%, and was considered to be quite high. Further research is needed to manufacture a more uniform coating layer in the future.

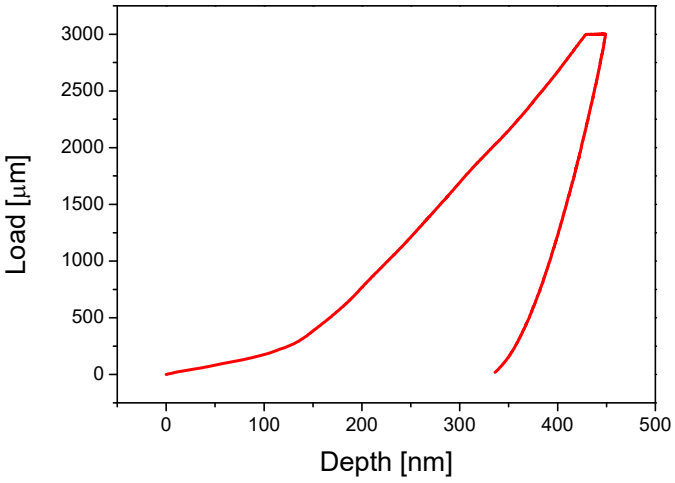

Fig. 4. Nano indentation result curve of APS coating layer

4. Conclusions

This study used the atmospheric plasma spray process to manufacture a MoO_3 coating layer, and presented the microstructure, phase composition, and properties of the manufactured coating layer. A sound MoO_3 coating layer was obtained using the process conditions of 600A, 45V. The cross-sectional microstructure of the coating layer was composed of lamellae, the typical APS process characteristic, and defects such as inter-lamellar cracks, large pores and unmelted powders were observed. Unlike the feedstock composition phase(α-MoO_3), the coating layer was composed of α-MoO_3, β-MoO_3, MoO_2. The phase transformation mechanism was identified to be caused by the rapid cooling that occurred during the process. Based on such findings, the possibility of manufacturing a MoO_3 coating layer using thermal spray was confirmed, and this process is anticipated to make a great to in manufacturing thick MoO_3 films.

Acknowledgments

This study was supported by Korea Institute for Advancement of Technology (KIAT) grant funded by the Korea Government (MOTIE) (No.20011286, The technology innovation program).

REFERENCES

[1] S.S. Mahajan, S.H. Mujawar, P.S. Shinde, A.I. Inamdar, P.S. Patil, Int. J. Electrochem. Sci. **3** (8), 953-960 (2008).
[2] J. Haber, E. Lalik, Catal. Today **33** (1-3), 119-137 (1997).
[3] A.A. Mane, A.V. Moholkar, Appl. Surf. Sci. **405**, 427-440 (2017).
[4] S.S. Sunu, E. Prabhu, V. Jayaraman, K.I. Gnanasekar, T.K. Seshagiri, T. Gnanasekaran, Sens. Actuators B Chem. **101** (1-2), 161-174 (2004).
[5] L. Zhou, L. Yang, P. Yuan, J. Zou, Y. Wu, C. Yu, J. Phys. Chem. C **114** (49), 21868-21872 (2010).
[6] A. Abdellaoui, L. Martin, A. Donnadieu, Phys. Status Solidi (a) **109** (2), 455-462 (1988).
[7] Q. Xiang, D. Zhang, J. Mater. Sci. Mater. Electron. **28** (10), 7449-7453 (2017).
[8] R. Sivakumar, P. Manisankar, M. Jayachandran, C. Sanjeeviraja, Sol. Energy Mater. Sol. Cells **90** (15), 2438-2448 (2006).
[9] M. Kharrazi, A. Azens, L. Kullman, C.G. Granqvist, Thin Solid Films **295** (1-2), 117-121 (1997).
[10] Y. Zhang, S. Kuai, Z. Wang, X. Hu, Appl. Surf. Sci. **165** (1), 56-59 (2000).
[11] J.R. Davis, Handbook of Thermal Spray Technology, ASM International (2004).
[12] G.J. Gill, R.C. Tucker, Mater. Sci. Technol. **2** (3), 207-213 (1986).
[13] M.C. Son, J.R. Park, K.T. Hong, H.K. Seok, Corros. Sci. Technol. **4** (1), 33-38 (2005).
[14] M. Golozar, K. Chien, T.W. Coyle, J. Therm. Spray Technol. **21** (3-4), 469-479 (2012).
[15] R.B. Anjaneyulu, B.S. Mohan, G.P Naidu, R. Muralikrishna, J. Asian Ceram. Soc. **6** (3), 183-195 (2018).
[16] D. Thirumalaikumarasamy, K.S. Kamalamoorthy, V.B. Visvalingam, J. Magnes. Alloy. **3** (3), 237-246 (2015).
[17] T. Gnaeupel-Herold, H.J. Prask, J. Barker, F.S. Biancaniello, R.D. Jiggetts, J. Matejicek, Mater. Sci. Eng. A **421** (1-2), 77-85 (2006).
[18] H. Myalska, J.K. Michalska, G. Moskal, K. Szymański, Surf. Coat. Technol. **318**, 270-278 (2017).
[19] L. Pawlowski, The science and engineering of thermal spray coatings, John Wiley & Sons (2008).
[20] M. Shahien, M. Yamada, T. Yasui, M. Fukumoto, Mater. Trans. T-M2012831 (2013).
[21] H.J. Kim, Y.J. Kim, J. Mater. Sci. **34** (1), 29-33 (1999).